Judd-Ofelt analysis and emission spectroscopy of Dy3+-doped InF3-based glass for visible fiber lasers

Jonathan Demaimay, Pavel Loiko, Thiphanie Rault, Solenn Cozic, Laurine Bodin, Elena Dunina, Liudmila Fomicheva, Alexey Kornienko, Patrice Camy, Ammar Hideur, et al.

Judd-Ofelt analysis and emission spectroscopy of Dy^{3+}-doped InF_3-based glass for visible fiber lasers

Jonathan Demaimay[a], Pavel Loiko[a,*], Thiphanie Rault[b], Solenn Cozic[b], Laurine Bodin[b], Elena Dunina[c], Liudmila Fomicheva[d], Alexey Kornienko[c], Patrice Camy[a], Ammar Hideur[e], and Alain Braud[a]

[a]Centre de Recherche sur les Ions, les Matériaux et la Photonique (CIMAP), UMR 6252 CEA-CNRS-ENSICAEN, Université de Caen Normandie, 6 Boulevard Maréchal Juin, 14050 Caen Cedex 4, France
[b]Le Verre Fluoré, rue Gabriel Voisin, Campus de Ker-Lann, 35170 Bruz, France
[c]Vitebsk State Technological University, 210035 Vitebsk, Belarus
[d]Belarusian State University of Informatics and Radioelectronics, 6 Brovka St., 220027, Minsk, Belarus
[e]CORIA UMR 6614, CNRS-INSA-Université de Rouen Normandie, 76801 Saint Etienne du Rouvray, France

ABSTRACT

We report a detailed spectroscopic investigation of Dy^{3+}-doped fluoroindate (InF_3-based) glass, aimed at assessing its suitability for visible laser applications. The *f–f* transition intensities were evaluated using a modified Judd–Ofelt theory incorporating configuration interaction effects: the radiative lifetime of the $^4F_{9/2}$ manifold is 1.32 ms and the luminescence branching ratio for the $^4F_{9/2} \rightarrow {}^6H_{13/2}$ transition amounts to 50.2%. The corresponding stimulated-emission cross section is 1.68×10^{-21} cm^2 at 574 nm (yellow emission). For a doping concentration of 0.5 mol% DyF_3, the luminescence lifetime is 1.23 ms, yielding a near-unity luminescence quantum efficiency. The resonant excited state absorption from the long-living terminal laser level is accounted by calculating the gain cross-section profiles indicating a gain bandwidth of ~10 nm. These results identify Dy^{3+}:InF_3 glass as a highly promising active medium for compact yellow fiber lasers and amplifiers.

Keywords: fluoride glasses; dysprosium ions; Judd-Ofelt theory; luminescence; visible laser.

1. INTRODUCTION

In ongoing research for novel laser sources emitting in the visible and mid-infrared spectral ranges, fluoride glasses have emerged as promising host materials due to their low phonon energies and wide transparency windows. Although ZrF_4-based (ZBLAN) glasses currently dominate this field, fluoroindate (InF_3-based) glasses offer several potential advantages, including lower phonon energy, improved rare-earth solubility, reduced concentration quenching, and extended infrared transparency [1–4]. Rare-earth-doped fluoroindate glasses are particularly suitable for efficient radiative transitions because the reduced multiphonon relaxation enhances the luminescence quantum yields. Dysprosium ions (Dy^{3+}) (electronic configuration [Xe]4f^9) are of special interest due to their strong yellow emission near 575 nm, corresponding to the $^4F_{9/2} \rightarrow {}^6H_{13/2}$ electronic transition, which enables compact solid-state and fiber laser sources in a spectral region where efficient emitters remain limited. Achieving laser emission in Dy^{3+}-doped materials, however, is challenging [5]. The weak absorption in the blue region, mainly associated with partially spin-forbidden transitions, limits pump efficiency, while cross-relaxation processes and reabsorption from the $^6H_{13/2}$ lower laser level reduce population inversion. Recently, fiber laser geometries have demonstrated significant progress for yellow Dy^{3+} lasers pumped by GaN laser diodes, as the long interaction lengths and low dopant concentrations help mitigate these limitations [6]. Despite the favourable properties of InF_3-based glasses, detailed spectroscopic investigations of Dy^{3+} in the visible spectral range remain relatively limited, particularly regarding absorption cross sections, gain characteristics, and the influence of reabsorption processes [7].

*e-mail: pavel.loiko@ensicaen.fr

In the present work, we report a comprehensive spectroscopic study of a fluoroindate glass doped with 0.5 mol% DyF_3. Absorption and emission properties are analysed, and the radiative parameters and gain cross sections relevant to visible laser operation are evaluated.

2. RAMAN SPECTROSCOPY

Fluoroindate glass doped with 0.5 mol% Dy^{3+} ions was fabricated by *Le Verre Fluoré*. The glass were prepared by the melting-quenching technique using high-purity fluoride starting materials which were melted in platinum crucibles at $T >$ 800 °C under dry atmosphere. To prevent crystallization, the homogeneous melt was rapidly cooled by casting onto a metallic mold. The glass was annealed near the glass transition temperature to remove mechanical stress.

The Raman spectrum of the studied Dy^{3+}:InF_3 glass is given in Fig. 1 and is compared to its ZrF_4 counterpart. It has been measured using a *Renishaw* Qontor confocal laser microscope equipped with a ×50 *Leica* objective and a 2400 gr/mm diffraction grating, using an Ar^+ ion laser (457 nm) as excitation source. The spectrum reveals two broad bands, indicating a disordered network with mixed bridging and non-bridging fluorine ions. The lower energy band at 150–350 cm^{-1} is assigned to the bending vibrations of the fluoroindate group while the most intense one spanning 350 to 600 cm^{-1} corresponds to the In–F stretching vibrations of InF_6 octahedra [8]. The asymmetry of the higher energy band possibly indicates to network modifier-fluorine bonds that fill the mid-frequency bands between 250 and 500 cm^{-1}. No sharp peaks are visible in the spectrum, attesting that the glass is fully amorphous and ruling out crystallization upon rare-earth doping. The maximum phonon frequency is 508 cm^{-1}, being lower as compared to ZBLAN glass (579 cm^{-1}).

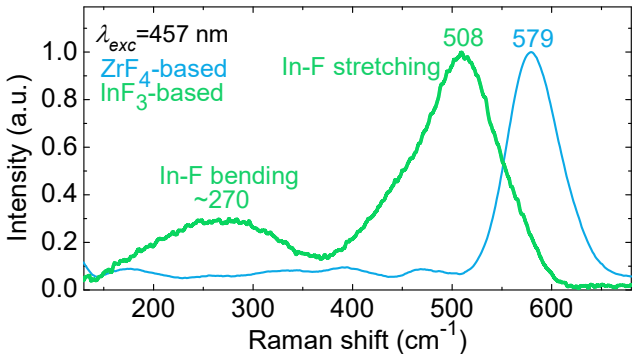

Figure 1. Raman spectra of Dy^{3+}-doped InF_3 and ZrF_4 based glasses, *numbers* – phonon energies in cm^{-1}, λ_{exc} = 457 nm.

3. ABSORPTION SPECTROSCOPY AND JUDD-OFELT THEORY

The absorption properties of Dy^{3+} ions in the InF_3-based glass were measured using a spectrophotometer (Cary 5000, *Agilent*), with a spectral bandwidth of 0.4 nm in the visible and 1.5 nm in the near-infrared. The absorption cross-sections, were obtained from the formula $\sigma_{abs} = \alpha_{abs} / N_{Dy}$, where α_{abs} is the absorption coefficient in cm^{-1}, and N_{Dy} is the doping concentration of Dy^{3+} ions ($N_{Dy} = 9.12\times10^{19}$ atoms/cm^3). The σ_{abs} spectra are depicted in Fig. 2.

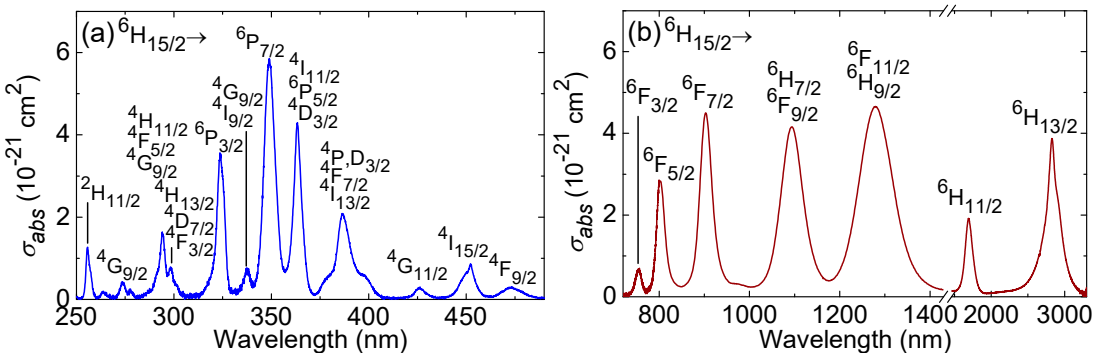

Figure 2. Absorption cross-sections, σ_{abs}, of Dy^{3+} ions in the InF_3-based glass in the (a) UV-blue and; (b) near-infrared spectral ranges.

In the UV-blue spectral range, the observed absorption bands arise from transitions from the ground state $^6H_{15/2}$ to the ^4F_J, ^4I_J, ^4G_J, ^4D_J, ^6P_J, ^4H_J, and ^2H_J excited manifolds, see Fig. 2(a). Among them, transitions terminating at the ^6P_J levels (J = 3/2, 5/2, and 7/2) are the most intense ones, due to their spin-allowed character ($\Delta S = 0$). The maximum absorption cross-section value is found for the $^6H_{15/2} \rightarrow {}^6P_{7/2}$ transition, $\sigma_{abs} = 5.85\times10^{-21}$ cm^2 at 348.8 nm. In the blue, the $^6H_{15/2} \rightarrow {}^4I_{15/2}$ transition exhibiting σ_{abs} of 0.86×10^{-21} cm^2 at 452.2 nm (absorption bandwidth: 5.0 nm) is suitable for pumping with GaN laser diodes emitting at 450 nm. In the near-infrared spectral range, absorption bands are associated to transitions from the ground-state to the higher-lying ^6F_J (J = 3/2, 5/2, 7/2, 9/2, and 11/2) and $^6H_{J'}$ (J' = 7/2, 9/2, 11/2, and 13/2) energy levels.

Based on the measured absorption spectra, *f–f* transition intensities of Dy^{3+} ions were analyzed in the framework of the Judd-Ofelt (J-O) theory. To improve the fitting of the experimental absorption oscillator strengths (f_{exp}), a parametrization scheme accounting for intermediate configuration interaction (ICI) was implemented [9,10]. The experimental and calculated (f^{Σ}_{calc}, Σ stands for ED + MD, ED – electric dipole, MD – magnetic dipole) absorption oscillator strengths obtained through both the standard theory and the ICI approximation are listed in Table 1. Here, $\langle E \rangle$ is the energy of the "center of gravity" of the absorption band, and Γ is the integrated absorption coefficient. The use of the former model provides lower root mean square (r.m.s) deviation between the f_{exp} and f^{Σ}_{calc} values.

Table 1. Intensities of transitions in absorption of Dy^{3+} ions in the InF_3-based glass

$^6H_{15/2}\rightarrow$	$\langle E \rangle$, cm^{-1}	Γ, cm^{-1}.nm	f^{Σ}, 10^{-6}		
			f_{exp}	f^{Σ}_{calc} (J-O)	f^{Σ}_{calc} (ICI)
$^6H_{13/2}$	3461.2	108.55	1.499	1.028^{ED}+ 0.336^{MD}	0.824^{ED}+ 0.336^{MD}
$^6H_{11/2}$	5897.3	28.041	1.080	0.958	1.126
$^6H_{9/2} + {}^6F_{11/2}$	7802.6	43.720	2.952	3.021	2.983
$^6F_{9/2} + {}^6H_{7/2}$	9146.7	24.0801	2.294	3.021	2.983
$^6H_{5/2} + {}^6F_{7/2}$	11070	16.600	2.249	2.371	2.382
$^6F_{5/2}$	12461	8.420	1.451	1.035	1.250
$^6F_{3/2} + {}^6F_{1/2}$	13270	2.911	0.543	0.197	0.239
$^4F_{9/2}$	21126	0.594	0.294	0.179	0.216
$^4I_{15/2}$	22204	0.784	0.427	0.356^{ED}+ 0.089^{MD}	0.498^{ED}+ 0.089^{MD}
$^4G_{11/2}$	23459	0.255	0.155	0.114	0.091
$^4F_{7/2} + {}^4I_{13/2} + {}^4M_{21/2} + {}^4K_{17/2}$	25828	2.762	2.031	2.204^{ED}+ 0.007^{MD}	2.690^{ED}+ 0.007^{MD}
$^4P_{5/2} + {}^4I_{11/2} + {}^4P_{7/2} + {}^4M_{15/2} + {}^4D_{5/2} + {}^4I_{9/2}$	28618	7.168	6.347	6.011^{ED}+ 0.011^{MD}	6.281^{ED}+ 0.011^{MD}
$^4G_{9/2} + {}^4P_{3/2} + {}^4M_{17/2}$	30809	1.758	2.62	0.950	1.386
$^4K_{13/2} + {}^4F_{3/2} + {}^4K_{13/2} + {}^4D_{7/2} + {}^4H_{11/2} + {}^4H_{9/2} + {}^4F_{5/2}$	33751	1.136	1.447	1.017^{ED}+ 0.015^{MD}	1.264^{ED} +0.015^{MD}
r.m.s. deviation				0.539	0.415

The sets of intensity parameters for the two models applied are $\Omega_2 = 0.139$, $\Omega_4 = 3.669$, and $\Omega_6 = 2.612$ [10^{-20} cm^2] for the standard parametrization scheme and $\Omega_2 = 2.309$, $\Omega_4 = 3.241$, $\Omega_6 = 3.625$ [10^{-20} cm^2], $R_2 = -0.215$, $R_4 = 0.228$ and $R_6 = 0.049$ [10^{-4} cm] for the ICI one.

The probabilities of spontaneous radiative transitions from the $^4F_{9/2}$ metastable state, $A^{\Sigma}_{calc}(JJ')$, were further calculated using the intensity parameters obtained within the ICI approximation. By using the total probability of radiative spontaneous transitions $A_{tot} = \Sigma_{J'} A^{\Sigma}_{calc}(JJ')$, the radiative lifetime $\tau_{rad} = 1/ A_{tot}$ as well as the luminescence branching ratios $\beta_{JJ'} = A^{\Sigma}_{calc}(JJ') / A_{tot}$ were computed. The results of the spontaneous radiative transition probabilities of Dy^{3+} ions are given in Table 2. Here, $\langle \lambda_{em} \rangle$ is the mean wavelength of the emission band predicted based o the energy barycenters of transitions in absorption. The analysis yielded a radiative lifetime of 1.32 ms for the $^4F_{9/2}$ manifold. The luminescence branching ratios $\beta_{JJ'}$ are 50.2% and 30.3 % for the $^4F_{9/2} \rightarrow {}^6H_{13/2}$ and $^4F_{9/2} \rightarrow {}^6H_{15/2}$ transitions, respectively, indicates a strong yellow emission and a balanced yellow-to-blue ratio, Y/B = 1.66, which is favorable to achieve near-white light emission and carries potential for high efficiency white light emitting phosphors [11].

Table 2. Calculated probabilities of spontaneous radiative transitions of Dy^{3+} ions in the Dy:InF_3 glass

$^4F_{9/2}\rightarrow$	$\langle\lambda_{em}\rangle$, nm	$A^{\Sigma}_{calc}(JJ')$, s^{-1}	$\beta_{JJ'}$, %	τ_{rad}, ms
$^6F_{1/2} + {}^6F_{3/2}$	1272.9	0.22^{ED}	0.03	1.23
$^6F_{5/2}$	1154.1	1.55^{ED}	0.2	
$^6H_{5/2} + {}^6F_{7/2}$	994.4	$10.37^{ED} + 4.29^{MD}$	1.93	
$^6H_{7/2} + {}^6F_{9/2}$	834.8	$28.38^{ED} + 6.96^{MD}$	4.66	
$^6H_{9/2} + {}^6F_{11/2}$	750.6	$24.56^{ED} + 42.02^{MD}$	8.78	
$^6H_{11/2}$	656.6	$20.60^{ED} + 9.63^{MD}$	3.99	
$^6H_{13/2}$	566.1	380.26^{ED}	50.16	
$^6H_{15/2}$	473.4	229.30^{ED}	30.25	

4. VISIBLE EMISSION SPECTROSCOPY

The luminescence spectrum of Dy^{3+} ions in the visible spectral range was measured using the confocal laser microscope. It exhibits four bands related to transitions from the $^4F_{9/2}$ metastable state to the lower-lying ^6H_J levels, (J = 15/2, 13/2, 11/2, 9/2) leading to cyan, yellow, red and deep-red emissions, respectively. The yellow emission centered at 573 nm is the most intense one. The corresponding emission bandwidth (FWHM) is 13 nm, being slightly broader than that for the ZrF_4 glass (12 nm). This can be explained by a broader distribution of local crystal fields around the dopant ions in InF_3 based glass, as well as more polarizable host lattice, contributing to enhanced inhomogeneous spectral line broadening.

The stimulated-emission (SE) cross-sections, σ_{SE}, of Dy^{3+} ions in the InF_3-based glass were calculated via the Füchtbauer–Ladenburg equation [12]:

$$\sigma_{SE}^{JJ'}(\lambda) = \frac{\lambda^5}{8\pi c \langle n\rangle^2 \tau_{rad}} \times \frac{\beta(JJ')W_{JJ}(\lambda)}{\int W_{JJ}(\lambda)d\lambda}, \quad (1)$$

where λ is the light wavelength, c is the speed of light, $\langle n\rangle \sim 1.49$ is the refractive index of the glass [1], τ_{rad} is the radiative lifetime of the emitting state, $\beta(JJ')$ is the luminescence branching ratio for the considered $J \rightarrow J'$ transition, and $W_i(\lambda)$ is the spectral profile of the considered emission band. The radiative transition probabilities obtained through the ICI theory were used in this calculation. The SE cross-section spectrum is depicted in Fig. 3(a).

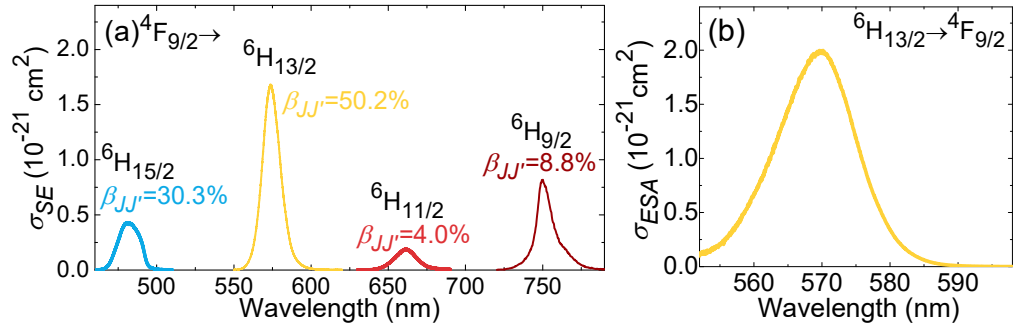

Figure 3. (a) Stimulated-emission cross-sections, σ_{SE}, of Dy^{3+} ions in the fluoroindate glass for transitions from the $^4F_{9/2}$ manifold to the $^6H_{15/2}$ (cyan), $^6H_{13/2}$ (yellow), $^6H_{11/2}$ (red), and $^6H_{9/2}$ (deep-red) ones; (b) excited-state absorption cross-sections, σ_{ESA}, for the $^6H_{13/2} \rightarrow {}^4F_{9/2}$ transition calculated using the reciprocity method.

The maximum σ_{SE} reaches 1.68×10^{-21} cm^2 at 573.8 nm for the $^4F_{9/2} \rightarrow {}^6H_{13/2}$ transition in the yellow, corresponding to an emission bandwidth of 13 nm, and for other colors, $\sigma_{SE} = 0.43\times10^{-21}$ cm^2 at 480.5 nm ($^4F_{9/2} \rightarrow {}^6H_{15/2}$), $\sigma_{SE} = 0.19\times10^{-21}$ cm^2 at 661.0 nm ($^4F_{9/2} \rightarrow {}^6H_{11/2}$), and $\sigma_{SE} = 0.82\times10^{-21}$ cm^2 at 750.2 nm ($^4F_{9/2} \rightarrow {}^6H_{9/2}$). The relatively high stimulated-emission cross-section indicates the suitability of the fluoroindate glass for efficient visible laser applications. The broad emission bandwidth is favorable for applications in tunable lasers, as well as amplifiers.

The $^6H_{13/2}$ level in the low-phonon-energy fluoroindate glass has a non-negligible lifetime (measured to be 0.65 ms for 0.5 mol% Dy^{3+} doping, by monitoring the 3 μm emission). It acts as the terminal laser level for the yellow transition, so that reabsorption via the resonant excited-state absorption (ESA) can significantly affect the net gain. The reciprocity method (McCumber formula) was used to estimate the σ_{ESA} spectral profile:

$$\sigma_{ESA} = \sigma_{SE} \times e^{\frac{h\upsilon - E_{ZPL}}{kT}}, \quad (2)$$

where h is the Planck constant, υ is the light frequency, and kT is the product of the Boltzmann constant k and the absolute temperature (T = 25 °C) [13]. The resulting σ_{ESA} spectrum in the yellow is presented in Fig. 3(b). It yields an estimation of the reabsorption cross section at the yellow emission wavelength of 1.42×10^{-21} cm^2 at 573.8 nm. The gain cross-section spectra for the yellow $^4F_{9/2} \rightarrow {}^6H_{13/2}$ transition with different population inversion ratios β are presented in Fig. 4, with $\sigma_{gain} = \beta\sigma_{SE} - (1-\beta) \times \sigma_{ESA}$. The resonant ESA is expected to slightly red shift the laser wavelength.

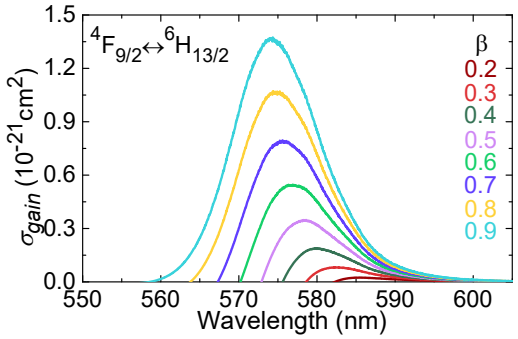

Figure 4. Gain cross-sections, σ_{gain}, for the $^4F_{9/2} \rightarrow {}^6H_{13/2}$ transition of Dy^{3+} ions in InF_3 based glass for different population inversions β.

The luminescence decay curve from the $^4F_{9/2}$ metastable manifold of Dy^{3+} ions is presented in Fig. 5. Its shape is indicative of energy transfer processes between Dy^{3+} ions, namely $^4F_{9/2} + {}^6H_{15/2} \rightarrow {}^6F_{1/2} + {}^6H_{9/2}$ or $^6F_{11/2}$; $^4F_{9/2} + {}^6H_{15/2} \rightarrow {}^6F_{5/2} + {}^6H_{5/2}$ and $^4F_{9/2} + {}^6H_{15/2} \rightarrow {}^6H_{9/2}$ or $^6F_{11/2} + {}^6F_{3/2}$. The mean luminescence lifetime amounts to 1.21 ms, corresponding to a luminescence quantum efficiency $\eta_q = \tau_{lum} / \tau_{rad}$ of 91.7%.

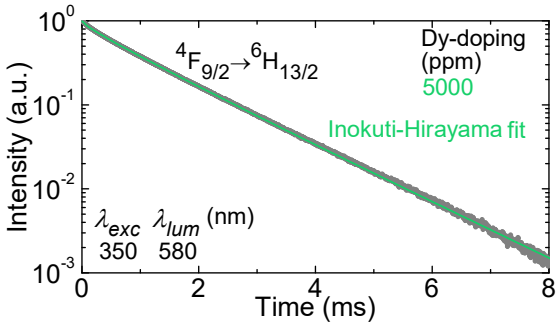

Figure 5. Luminescence decay curve from the $^4F_{9/2}$ metastable state of Dy^{3+} ions in the fluoroindate glass, *points* – experimental data, *curve* – their fit obtained by the Inokuti-Hirayama model.

A fit of the luminescence decay curve was provided using the Inokuti-Hirayama model [14] for multipolar interactions:

$$I(t) = I_0 \times \exp\left(\frac{t}{\tau_0} - \frac{4}{3}\pi R_0{}^3 N \times \Gamma\left(1-\frac{3}{s}\right) \times \left(\frac{t}{\tau_0}\right)^{\frac{3}{s}}\right), \quad (3)$$

where I is the luminescence intensity, t is time, τ_0 is the intrinsic luminescence lifetime (without interactions between Dy^{3+} ions), R_0 is the critical radius at which the probability of radiative and cross-relaxation processes become equal, N is the ion density, Γ is the gamma function, and s is a parameter indicating the character of interactions between the active ions. The best fit is obtained for a value of s = 6 which accounts for dipole-dipole interactions and yields a value for τ_0 of 1.38 ms.

5. CONCLUSIONS

To conclude, Dy^{3+} ions in fluoroindate glass combine broad absorption in the blue, around 450 nm, intense and wide emission in the yellow (σ_{SE} = 1.68×10^{-21} cm^2 at 573.8 nm, luminescence branching ratio: 50.2%), as well as a high luminescence quantum efficiency of >91% and a long luminescence lifetime of 1.21 ms. These features make it attractive

for the development of visible fiber lasers and amplifiers directly pumped by blue GaN diode lasers. The fiber geometry in this case will resolve the problem of relatively weak absorption in the blue originating from the spin forbidden nature of the corresponding optical transitions. From the material point of view, optimization of Dy^{3+} content may help to find a compromise between excessive self-quenching of luminescence via cross-relaxation and enhanced pump absorption. Codoping of the glass with Tb^{3+} ions may be considered as a way to quench the $^6H_{13/2}$ manifold in order to improve yellow laser efficiency and avoid self-pulsing common for Dy visible lasers.

6. ACKNOWLEDGEMENTS

This research received funding from Agence Nationale de la Recherche, France (projects NOVELA – ANR-22-CE08-0025-01 and LOVINOV – ANR-23-LCV2-0001), Région Normandie (Contrat de plan État-Région (CPER)).

REFERENCES

[1] P. P. Fedorov, R. M. Zakalyukin, L. N. Ignat'eva, and V. M. Bouznik, "Fluoroindate glasses," *Russ. Chem. Rev.* **69**(8), 705–716 (2000). https://doi.org/10.1070/RC2000v069n08ABEH000582

[2] L. Zhang, F. Guan, L. Zhang, and Y. Jiang, "Next generation mid-infrared fiber: fluoroindate glass fiber," *Opt. Mater. Express* **12**(4), 1683–1707 (2022). https://doi.org/10.1364/OME.454418

[3] S. Tanabe, T. Hanada, M. Watanabe, T. Hayashi, and N. Soga, "Optical properties of dysprosium-doped low-phonon-energy glasses for a potential 1.3 μm optical amplifier," *J. Am. Ceram. Soc.* **78**(11), 2917–2922 (1995). https://doi.org/10.1111/j.1151-2916.1995.tb09064.x

[4] Ł. Sójka, B. Starzyk, S. Sujecki, Ł. Pajewski, P. Miluski, J. Żmojda, W. A. Pisarski, J. Pisarska, M. Kochanowicz, D. J. Dorosz, T. M. Benson, D. Furniss, M. C. Farries, and A. B. Seddon, "Mid-infrared emission from Dy^{3+}-doped fluoroindate glass fiber," *Ceram. Int.* **49**(24 Pt B), 41210–41216 (2023). https://doi.org/10.1016/j.ceramint.2023.03.075

[5] Y. Ososkov, J. Lee, T. T. Fernandez, A. Fuerbach, and S. D. Jackson, "High-efficiency fluoroindate glass fiber laser," *Opt. Lett.* **48**(10), 2664–2667 (2023). https://doi.org/10.1364/OL.486318

[6] J. Lee, Y. Ososkov, T. T. Fernandez, A. Fuerbach, and S. D. Jackson, "Visible light generation and lasing from a fluoroindate glass fiber," *Opt. Lett.* **49**(4), 964–967 (2024). https://doi.org/10.1364/OL.515110

[7] J. Demaimay, E. Kifle, P. Loiko, F. Pau, G. Recoque, T. Georges, T. Rault, L. Bodin, P. Camy, and A. Braud, "Efficient yellow Dy:ZBLAN fiber laser with high-brightness diode-pumping at 450 nm," *Opt. Lett.* **49**(15), 4174–4177 (2024). https://doi.org/10.1364/OL.529025

[8] R. M. Almeida, J. C. Pereira, Y. Messaddeq, and M. A. Aegerter, "Vibrational spectra and structure of fluoroindate glasses," *J. Non-Cryst. Solids* 161, 105–108 (1993). https://doi.org/10.1016/0022-3093(93)90553-R

[9] A. A. Kornienko, A. A. Kaminskii, and E. B. Dunina, "Dependence of the line strength of f–f transitions on the manifold energy. II. Analysis of Pr^{3+} in $KPrP_4O_{12}$," *Phys. Status Solidi B* **157**(1), 267–273 (1990). https://doi.org/10.1002/pssb.2221570130

[10] P. Loiko, A. Volokitina, X. Mateos, E. Dunina, A. Kornienko, E. Vilejshikova, M. Aguiló, and F. Diaz, "Spectroscopy of Tb^{3+} ions in monoclinic $KLu(WO_4)_2$ crystal: application of an intermediate configuration interaction theory," *Opt. Mater.* **78**, 495–501 (2018). https://doi.org/10.1016/j.optmat.2018.02.043

[11] P. Shrivastava, J. Kaur, and V. Dubey, "White light emission by Dy^{3+} doped phosphor matrices: a short review," *J. Fluoresc.* **26**(1), 105–111 (2016).

[12] B. Aull and H. Jenssen, "Vibronic interactions in Nd:YAG resulting in nonreciprocity of absorption and stimulated emission cross sections," *IEEE J. Quantum Electron.* **18**(5), 925–930 (1982). https://doi.org/10.1109/JQE.1982.1071527

[13] W. H. McCumber, "Einstein relations connecting broadband emission and absorption spectra," *Phys. Rev.* **136**(4A), A954–A957 (1964). https://doi.org/10.1103/PhysRev.136.A954

[14] M. Inokuti and F. Hirayama, "Influence of energy transfer by the exchange mechanism on donor luminescence," *J. Chem. Phys.* **43**(6), 1978–1989 (1965). https://doi.org/10.1063/1.1697063